View Article Online / Journal Homepage / Table of Contents for this issue

A direct method for the preparation of glycolipid–metal nanoparticle conjugates: sophorolipids as reducing and capping agents for the synthesis of water re-dispersible silver nanoparticles and their antibacterial activity†

Sanjay Singh,[a] Pitamber Patel,[b] Swarna Jaiswal,[a] A. A. Prabhune,*[c] C. V. Ramana*[b] and B. L. V. Prasad*[a]

Received (in Durham, UK) 10th July 2008, Accepted 27th October 2008
First published as an Advance Article on the web 12th December 2008
DOI: 10.1039/b811829a

Published on 12 December 2008 on http://pubs.rsc.org | doi:10.1039/B811829A
Downloaded by University of Belgrade on 02 January 2013

The production of a new class of glycolipid–metal nanoparticle conjugates, namely, sophorolipid reduced/capped silver nanoparticles is demonstrated for the first time, by unveiling the reducing and capping abilities of sophorolipid derived from oleic acid. It is also demonstrated that the sophorolipid capped Ag nanoparticles are highly potent antibacterial agents, against both Gram-positive and Gram-negative bacteria. The utilization of sophorolipid brings out several advantages, such as eliminating the necessity for exogenous reducing agent and imparting better stability to the silver nanoparticles as compared to their oleic acid capped analogues. These sophorolipid capped silver nanoparticles can be obtained as a stable powder that can be re-dispersed in water as desired.

Introduction

Glycolipid conjugated nanoparticles—nanoparticles covered with carbohydrates bearing a long alkyl chain—are assuming great significance these days as models of carbohydrate–protein interactions, for their biomedicinal attributes and numerous other applications.[1] So far the protocols adopted for realizing such conjugates have relied on the traditional organic chemistry syntheses for preparation of the glycolipids and the standard reported methods for obtaining nanoparticles. For example, reduction of a metal ion by an appropriate reducing agent in the presence of the glycolipid or a post synthetic conjugation of these metal nanoparticles with a glycolipid concludes the preparation of a glycolipid–metal nanoparticle conjugate. Metal,[2] mostly dominated by gold, magnetic[3] and semi-conducting nanoparticles[4] have been the preferred nanosystems while a whole variety of carbohydrates ranging from simple monosaccharides to various oligosaccharides have been considered. While the nanosystems possess size dependent optoelectronic, magnetic and fluorescent properties, the carbohydrates bring on board biocompatibility, selective interactions with various proteins and molecules, and render the conjugates water dispersible. The last one is an important stipulation for any application related to biology of such highly functional conjugates.[5]

Silver metal nanoparticles (AgNPs) need a special mention in this regard, as they exhibit excellent toxicity towards various microorganisms in addition to attractive physiochemical properties.[6] Germicidal properties of Ag and AgNPs have been applied in water purification,[7] wound dressings (fabric impregnated with silver, FIS),[8] and as inhibitors of the HIV virus.[9] Potential antibacterial polyelectrolyte capsules[10] and nanocomposites consisting of a cationic polymer matrix with embedded silver bromide nanoparticles[11] have also been reported. Whilst the use of AgNPs for bio-related applications is well recognized, the important water dispersibility proviso has been generally achieved by using water soluble polymers,[12] oligo- and polysaccharides[13] as capping agents, whereas the reduction is in general carried out by citric acid salts,[14] sodium borohydride,[15] elemental hydrogen[16] or by alkaline amino acids[17] or polyol[18] solutions. A few reports have also appeared in which the reduction and stabilization is achieved by saccharides *via* a modified Tollens process.[19]

In this context we envisaged that the reduction of silver ions by employing a class of glycolipid bio-surfactants with proven microbial activity should address the aqueous silver nanoparticle synthesis and capping in one go, synergetic biological activity being exhibited for the derived AgNPs. Sophorolipids (SLs) that have been considered in this context for their established biocompatibility and antimicrobial, antifungal and antiviral activities consist of a dimeric glucose "*sophorose*" linked by a glycosidic bond to the penultimate carbon of the fatty acid and are accessible by simple biological means.[20,21] Herein, we disclose the dual capability of sophorolipids (such as reduction and capping), resulting in

[a] *Materials Chemistry Division, National Chemical Laboratory, Pune 411 008, India. E-mail: pl.bhagavatula@ncl.res.in*
[b] *Organic Chemistry Division, National Chemical Laboratory, Pune 411 008, India. E-mail: vr.chepuri@ncl.res.in*
[c] *Biochemistry Division, National Chemical Laboratory, Pune 411 008, India. E-mail: aa.prabhune@ncl.res.in; Fax: +91 20 25902636; Tel: +91 20 25902013*

† Electronic supplementary information (ESI) available: Synthetic and spectral details of acidic sophorolipid, comparison of UV-Vis spectra of re-dispersed oleic acid capped and sophorolipid capped nanoparticles, antibacterial properties of pure sophorolipid, photographs of plates showing the growth/inhibition of bacteria under different conditions. See DOI: 10.1039/b811829a

 This journal is © The Royal Society of Chemistry and the Centre National de la Recherche Scientifique 2009

Published on 12 December 2008 on http://pubs.rsc.org | doi:10.1039/B811829A
Downloaded by University of Belgrade on 02 January 2013

water dispersible AgNPs. Detailed investigation on the antimicrobial activity of the as synthesized AgNPs in comparison with the pure SL molecules is described.

Experimental section

Materials and methods

Silver nitrate ($AgNO_3$) and potassium hydroxide (KOH) were purchased from SRL, India. All the bacterial species were grown in Luria–Bertini (LB) medium and Agar purchased from HiMedia (Mumbai, India) and used as received. Oleic acid (99%) from Aldrich and glucose from HiMedia were used as received.

Synthesis of sophorolipid (SL)

In a 500 mL Erlenmeyer flask, *Candida bombicola* (ATCC 22214) was grown in MGYP nutrient medium for 48 h under shaking conditions (200 rpm) at 30 °C. The biomass was harvested by centrifugation (5000 rpm, 10 min) and was further dispersed with 2 mL of oleic acid solution (1 mL oleic acid in 1 mL ethanol). To this a solution of 10 wt% glucose in 100 mL water was added. The flask was incubated for 96 h under shaking conditions (200 rpm) at 30 °C. A brown coloured, thick viscous liquid (sophorolipid mixture) was isolated from the base of the flask and was further purified and characterized by reported methods (see electronic supporting information ESI-1†).[21a,21g,22]

Synthesis and purification of sophorolipid-reduced AgNPs (SL-AgNPs)

In a typical experiment, 100 mL of 10^{-3} M aqueous $AgNO_3$ solution were taken with 10^{-3} M purified acidic sophorolipid. To this solution, 1 mL of 1 M KOH solution (pH ~10) was added and the mixture was allowed to boil for about 5–10 min. The colourless solution turned yellow, which indicated the formation of AgNPs. In order to prove that the reduction occurred only at alkaline pH, a control experiment was set up in which the above reaction was carried out without the addition of KOH. It was observed that AgNPs did not form under neutral and acidic conditions. In another control experiment the above reaction was performed with $AgNO_3$ and KOH without the addition of SL and it was again observed that even after prolonged boiling there was no formation of AgNPs. This clearly indicates the crucial role of SL as a pH dependent reducing agent for the synthesis of AgNPs.

Subsequent to the synthesis the samples were dialyzed for 24 h by changing the water intermittently and then centrifuged at 15 000 rpm. This resulted in a thick pellet that was separated. The pellet was re-dispersed in water and centrifuged again. This process was repeated thrice and the final resultant pellet was spread in a Petri dish and air dried. The powder was collected and used for further analysis like TGA, UV-Vis (for re-dispersion experiments), FTIR and antibacterial studies.

For NMR characterizations a large quantity of the sample in 1000 mL volume was prepared. It was dialyzed as above and the sample was lyophilized. The obtained powder was re-suspended in D_2O and NMR characterizations were done.

Sample characterizations

UV-Vis spectra of SL-AgNPs were monitored on a Jasco-V-570 UV/Vis/NIR spectrophotometer operated at a resolution of 2 nm. ^1H and ^{13}C NMR spectroscopy measurements were carried out on a Bruker DRX 400 MHz spectrometer. The purified powders of SL and SL-AgNPs were crushed with KBr, pelleted and the Fourier transform infra-red (FTIR) spectra were recorded on a Perkin-Elmer Spectrum One instrument at a resolution of 4 cm^{-1}. Optical rotations were determined on a Jasco DIP-370 digital polarimeter. Specific optical rotations $[\alpha]_D$ are given in 10^{-1} deg cm^2 g^{-1}. Mass spectroscopy (EI, 70 eV, direct inlet system) was carried out on a Finnigan MAT-1020 spectrometer. Elemental analysis data were obtained on a Thermo Finnigan Flash EA 1112 Series CHNS Analyser. Samples for transmission electron microscopy (TEM) were prepared by drop coating the isolated and re-suspended solution on carbon-coated copper grids. TEM measurements were performed on Tecnai F 30 instrument operated at an accelerating voltage of 300 kV. X-ray diffraction (XRD) measurements of drop coated films of the SL-AgNPs on a glass substrate were carried out on X'Pert Pro by Panalytical instruments operated at a voltage of 40 kV and a current of 30 mA with Cu Kα radiation. Thermogravimetric analysis (TGA) of purified powders of dried SL-AgNPs was performed on a TGA-7 Perkin-Elmer instrument at a scan rate of 10 °C min^{-1}. Atomic force microscope (AFM) imaging of bacterial cells was performed in the contact mode using a VEECO Digital Instruments multimode scanning probe microscope equipped with a Nanoscope IV controller.

Testing of antibacterial properties

Before performing the antibacterial experiment, the re-suspended SL-AgNPs were dialyzed with a 12.5 kDa dialysis membrane for 24 h against a copious amount of deionized water in order to remove excess SL and unreduced Ag^+ ions. The SL-AgNPs were then autoclaved for 20 min.

Bacillus subtilis (ATCC 6633, Gram-positive bacterium), *Staphylococcus aureus* (ATCC 2079, Gram-positive bacterium) and *Pseudomonas aeruginosa* (ATCC 2207, Gram-negative bacterium) were used for initial antibacterial tests of SL alone, following an agar-well diffusion method (AWDM) as well as a standard dilution micromethod. Pre-inoculums of the above-mentioned bacterial strains were inoculated separately in 100 mL of Luria–Bertini medium and incubated (30 °C, 200 rpm) for 24 h in order to perform further experiments. For AWDM, 75 μL of the three above-mentioned bacterial strains were mixed gently in three different warm (~45 °C) and molten Luria–Bertini Agar solutions (20 mL). These solutions were then poured into three different sterile plates. Wells (7 mm in diameter) were punched in each agar plate using a sterile stainless steel borer. Each well was filled with 100 μL of different concentrations (0.5, 1 and 10%) of SL. The plates were incubated at 30 °C for 48 h. The diameters of the inhibitory zones were measured in mm.

Antibacterial tests for purified oleic acid capped and SL-AgNPs were performed using a standard dilution micromethod. The SL-AgNPs were diluted to 5, 10, 20, 40, 60, 80 and 100 μg mL^{-1} with sterile Millipore water. *Bacillus*

Published on 12 December 2008 on http://pubs.rsc.org | doi:10.1039/B811829A
Downloaded by University of Belgrade on 02 January 2013

subtilis was added to each of these dilutions of SL-AgNPs, at a concentration of 10^6 CFU mL^{-1}, and incubated for 12 h under shaking conditions. Aliquots of 100 μL were taken at different time intervals from the above solutions (*Bacillus subtilis* and SL-AgNPs) and plated on Luria–Bertini Agar plates. The plates were kept for 24 h at 30 °C and bacterial colonies were counted manually. Simultaneously, 100 μL samples were withdrawn from each of the above solutions and drop cast on freshly peeled off mica chips, then dried in a dust free environment at room temperature for AFM analysis. For antibacterial activity assessment against Gram-negative bacterial species, SL-AgNPs were diluted to 5, 10, 20, 40, 60 and 100 μg mL^{-1} and the rest of the experimental conditions were kept the same except for the bacterial species, as *Pseudomonas aeruginosa* was taken.

While performing antibacterial tests for purified SL against *Bacillus subtilis* and *Pseudomonas aeruginosa*, a range of sophorolipid concentrations (0.25, 0.50, 0.75 and 1.0 μg mL^{-1}) was taken with bacterial species at a concentration of 10^5 CFU mL^{-1}. Aliquots of 100 μL were taken at different time intervals from the above solutions (bacteria and sophorolipid) and plated on Luria–Bertini Agar plates. The plates were kept for 24 h and incubated at 30 °C. The bacterial colonies were then counted manually. Simultaneously, 100 μL samples were withdrawn from each of the above solutions and drop cast on freshly peeled off mica chips, then dried in a dust free environment at room temperature for AFM analysis.

Lipid peroxidation (LPO) reaction

Formation of malondialdehyde (MDA) was used as an index to measure lipid peroxidation. MDA was quantified based on its reaction with thiobarbituric acid (TBA) to form a pink MDA–TBA adduct,[23] which shows absorbance at 532 nm. 1 mL of bacterial cells treated with SL-AgNPs was mixed with 2 mL of 10% (wt/vol) trichloroacetic acid, and the solids were removed by centrifugation at 11 000 rpm for 35 min and then for an additional 20 min to ensure that the SL-AgNPs, cells, and precipitated proteins were completely removed. Three millilitres of a freshly prepared 0.67% (wt/vol) TBA (Sigma Chemical Co.) solution were then added to the supernatant. The samples were incubated in a boiling water bath for 10 min and cooled, and the absorbance at 532 nm was measured on a Jasco V-570 UV/Vis/NIR spectrophotometer operated at a resolution of 2 nm.

Results and discussion

Sophorolipids are known to result through a multi-step pathway when glucose and a fatty acid are provided in the growth medium of specific yeast strains.[20a] We obtained acidic sophorolipid [Fig. 1A] by following a literature procedure[21g] and the details have already been reported.[22] All the spectroscopic characterizations (ESI-1†) are in complete agreement with the reported literature,[21g] supporting the formation of a pure acidic form of SL. After a substantial optimization of the experimental parameters, reduction of silver ions was concluded successfully by heating equimolar (10^{-3} M) silver nitrate and SL in alkaline solution (1 M KOH). The reduction was instantaneous and the AgNPs were isolated as a stable powder by simple centrifuging and air-drying. Fig. 1B shows UV-Vis spectra recorded from aqueous solutions of silver nitrate and SL at neutral pH conditions (curve-1), silver nitrate and KOH (curve-2), alkaline solution of silver nitrate and SL (curve-3) and re-dispersed AgNPs (curve-4). It is obvious from the control experiments (curves-1 and -2) that both SL and KOH with silver nitrate are essential for the synthesis of AgNPs. The strong absorption with a peak at *ca.* 410 nm (curve-3) clearly indicates the formation of AgNPs. This absorption is due to excitation of surface plasmons present in the nanoparticles and the peak width and position observed clearly indicate the particles to be in the 10–50 nm size range which was further corroborated by TEM analysis (*vide infra*).[24] The SL-AgNPs are stable for several months in solution. Simple centrifuging resulted in the separation of particles from solution and the separated pellet could be dried at room temperature to obtain the SL-AgNPs in powder form. This powder can be easily re-dispersed in water. The surface plasmon peak position (curve-4) from this re-dispersed solution is at a similar value to that observed in as prepared SL-AgNPs and the minor broadening is attributed to some aggregation during solvent evaporation.

Transmission electron microscope (Fig. 2A and B) images from as synthesized SL-AgNPs revealed the average particle size to be ~15 nm (inset, Fig. 2A). The selected area electron diffraction (SAED) pattern (inset, Fig. 2B) shows that the particles are polycrystalline in nature with the diffraction rings indexed to face-centred cubic (fcc) structure of silver.[25] The well-defined intense Bragg reflections characteristic of fcc silver are seen in the XRD pattern (Fig. 2C). TGA analysis (Fig. 2D) of SL-AgNPs indicated about 20% weight loss in two steps, one around 200 °C (~10% weight loss) and the

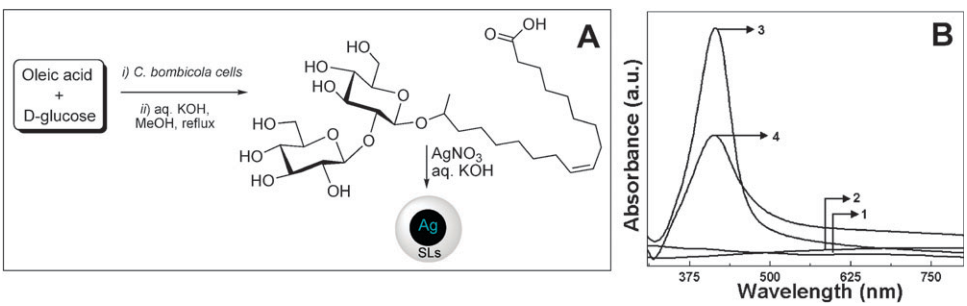

Fig. 1 (A) Synthesis scheme of sophorolipid and SL-AgNPs. (B) UV-Vis of aq. mixture of silver nitrate and sophorolipid (curve-1), mixture of silver nitrate and KOH (curve-2), as prepared SL-AgNPs (curve-3) and SL-AgNPs re-dispersed in water (curve-4).

 This journal is © The Royal Society of Chemistry and the Centre National de la Recherche Scientifique 2009

Published on 12 December 2008 on http://pubs.rsc.org | doi:10.1039/B811829A
Downloaded by University of Belgrade on 02 January 2013

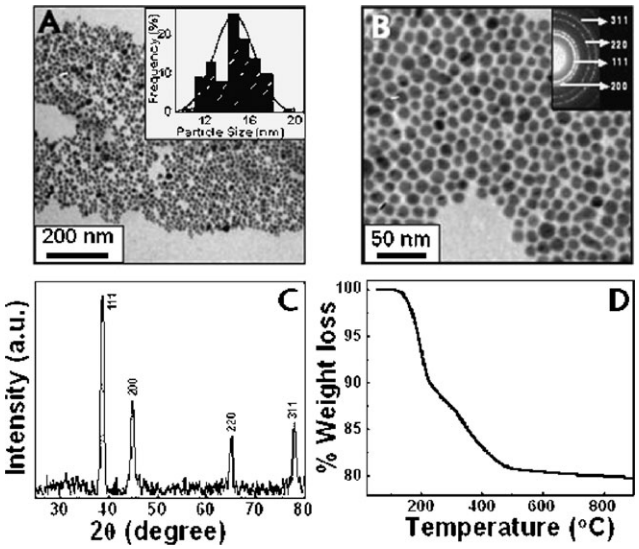

Fig. 2 (A and B) TEM images of SL-AgNPs. The insets in (A) and (B) show the particle size distribution and the selected area electron diffraction respectively. (C) Powder XRD pattern of SL-AgNPs. The peaks are indexed to fcc phase of silver. (D) Thermogravimetric analysis of SL-AgNPs.

other around 330 °C (~10% weight loss). This is slightly higher than the expected weight loss for a ligand, capping a 15 nm diameter particle in a monolayer fashion (~16%),[26] thus indicating either denser ligand (SL) packing on a 3D surface or packing in multilayers.

We believe a mechanism similar to that of polyol mediated reduction of silver salts[18] is operative in the present case considering the availability of several free hydroxyl groups in sophorolipid. Consequently, to probe the nature of ligand capping on nanoparticle surfaces we examined the SL-AgNPs by FTIR and NMR spectroscopy. The comparative FTIR spectra of pure SL and SL-AgNPs are presented in Fig. 3A. The carbonyl (region-I) and olefin (region-II) regions are marked and enlarged in the accompanying panels. The –C═O stretch (1709 cm^{-1}, region-I) in pure SL is shifted to 1574 cm^{-1}, indicating its binding to the AgNPs surface. The association of –C═C– with the AgNPs surface is evident from the region-2 where olefinic–H stretching frequency at 3004 cm^{-1} is absent.[27] The binding through –C═C– to the nanoparticle surface is also supported by ^{1}H NMR spectroscopy (Fig. 3B, D_2O as solvent).‡ Here the spectra of SL capped AgNPs (curve 2, Fig. 3B) clearly display a downfield shift of the olefinic proton (Δ_δ = 0.16 ppm) as compared to that in pure sophorolipid (curve 1, Fig. 3B).[28] Nevertheless, the possibility of some SL binding to the NP surface through the –COOH group is not ruled out. It should be noted, however, that in either case (–CO_2H or –C═C– binding to nanoparticle surface), hydrophilic disaccharide units form the exterior of AgNPs, thus ensuing their water dispersibility. Conversely, oleic acid capping on the nanoparticle surface is known to depend on the solvent environment, as reported in detail by Efrima's group.[27] They concluded that in an aqueous environment the

‡ Please note that these spectra are taken in D_2O as compared to the CD_3OD–$CDCl_3$ mixture that was used for the data presented in the electronic supporting information.†

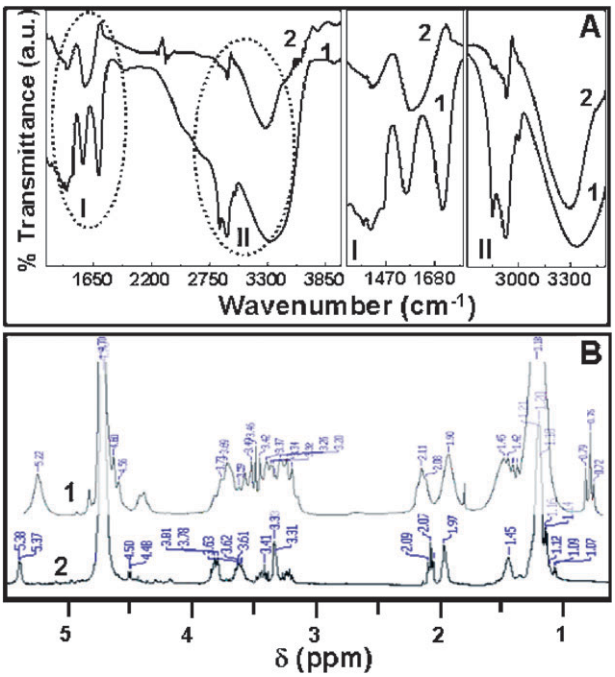

Fig. 3 (A) FTIR spectra of pure sophorolipid (1) and sophorolipid capped silver nanoparticles (2). The regions 1400–1700 cm^{-1} and 2700–3500 cm^{-1} are marked I and II and are enlarged in the accompanying panels. (B) ^{1}H NMR spectra of pure sophorolipid (1) and of sophorolipid capped AgNPs (2).

binding of oleic acid to the surface of AgNPs takes place through the double bond while in an organic environment the –COOH group participates in the binding. As compared to the SL-AgNPs, simple centrifugation and drying out of oleic acid capped AgNPs (OA-AgNPs) resulted in irreversible aggregation, as substantiated by a broadened surface plasmon resonance peak after re-dispersion (Electronic supporting information; ESI-Fig-1, curve-d†). Though aqueous OA-AgNPs could be obtained as powder by salt induced precipitation[29] these also undergo irreversible aggregation on removal of salt ions by dialysis. Moreover, as oleic acid is not soluble in water, for making OA-AgNPs we need to disperse oleic acid in a water–alcohol mixture and being just a capping agent, realization of OA-AgNPs also necessitates the addition of an exogenous reducing agent like citrate or borohydride. All these clearly exemplify the advantage of sophorolipid over oleic acid for the synthesis of silver nanoparticles.

Antibacterial activity

The preliminary comparative antibacterial activity of SL was assessed against *Bacillus subtilis*, *Staphylococcus aureus* and *Pseudomonas aeruginosa* by an agar well diffusion method (ESI-Fig-2†). A well-defined zone of inhibition was observed at all the concentrations tested in the case of Gram-positive bacteria: *Bacillus subtilis* (ESI-Fig-2; Plate A†) and *Staphylococcus aureus* (ESI-Fig-2; Plate B†), while there was a faint zone of inhibition seen only at 10 wt% in the case of Gram-negative bacteria: *Pseudomonas aeruginosa* (ESI-Fig-2; Plate C†). It has been reported that pure SL is not very effective against Gram-negative bacteria[21i] and our results are in accordance with this. In contrast, silver is known to be a

Published on 12 December 2008 on http://pubs.rsc.org | doi:10.1039/B811829A
Downloaded by University of Belgrade on 02 January 2013

broad spectrum bactericidal agent.[19a] Thus it remains to be seen whether SL capping on AgNPs would show any effect on the latter's antibacterial activity. To address this, the antibacterial activity of SL-AgNPs was assessed with *Bacillus subtilis* (Gram-positive) and *Pseudomonas aeruginosa* (Gram-negative).

A range of SL-AgNPs concentrations (20, 40, 60, 80 and 100 μg mL^{-1}) were exposed to *Bacillus subtilis* for varying time periods. These concentrations of SL-AgNPs were chosen based on several earlier reports.[13,19a] In all the cases the cell survival dropped dramatically to lower than 0.4% within an hour of exposure (Fig. 4A). Compared to the initial concentrations of the bacterial cells taken, this survival is effectively nil. The respective plate images (ESI-Fig-3†) show the extent of antibacterial activity of the different concentrations of SL-AgNPs exposed for different time intervals. Taking into account that pure SL are not effective bactericides against Gram-negative bacteria,[21i] we did the experiments with SL-AgNPs on Gram-negative bacteria rather circumspectly with the same concentrations of SL-AgNPs as above, namely 20, 40, 60 and 100 μg mL^{-1}. Quite surprisingly, the SL-AgNPs are very effective and the cells of *Pseudomonas aeruginosa* showed no survival at these concentrations (ESI-Fig-4†). Therefore in order to get some statistical data we reduced the concentrations of SL-AgNPs and repeated the experiments. Here, SL-AgNPs concentrations of 5 and 10 μg mL^{-1} exhibited cell survival of 0.03% and 0.008% respectively (Fig. 4B and ESI-Fig-5†). In fact Gram-positive bacteria showed much better survival instincts (~30%) at these lower concentrations (5 and 10 μg mL^{-1}; ESI-Fig-6†), making it very clear that SL-AgNPs are more effective bactericidal agents against Gram-negative bacteria. AFM images of *Bacillus subtilis* (Fig. 5A–C) show cells having intact features and those treated with SL-AgNPs show complete disintegration of the cell membrane (Fig. 5D–F) leading to leakage of cytoplasmic material.[30] The appearance of high contrast regions in the AFM images could be attributed to the presence of dense cytoplasmic material. Similar results are observed in the case of *Pseudomonas aeruginosa* as well, with untreated bacterial cells (Fig. 6A–C) being intact and treated cells becoming smaller in size with increased roughening of the cell surface (Fig. 6D–F).

Since pure SL is reported to possess antibacterial activity, proving that the capped SL alone does not cause the antibacterial effects becomes mandatory in this context. The amount of SL capping to the AgNPs was calculated on the basis of TGA results and a similar amount of pure SL (ranging in concentration from 0.25 to 1 μg mL^{-1} corresponding to 1 to 5 μg mL^{-1} of SL-AgNPs) was used for testing the antibacterial activity against *Bacillus subtilis* (ESI-Fig-7†) and *Pseudomonas aeruginosa* (ESI-Fig-8†). It was observed that bacterial cells were unaffected by these concentrations of SL attesting to the fact that SL at these concentrations is not an effective bactericide and silver is causative of the antibacterial effects observed. This clearly proves that the SL capping does not hinder the availability/release of Ag^+ ions for the antibacterial activity.

Two main hypotheses for the mechanism of silver bactericidal activity have been put forward. One is the ability of silver to cause pore formation in bacterial cell membrane through the formation of reactive oxygen species (ROS) in the vicinity of the bacterial cell membrane and thus increase cell permeability and cell death.[31] The second one is related to the thin layer of Ag^+ ions present on the nanoparticle surface or their slow release from the AgNPs itself, that interact with DNA and various cellular enzymes by coordinating to electron donating groups such as thiols, carboxylates, amides, hydroxyls, imidazoles, indoles *etc.*[19a,32] While the damage to the cell membrane leads to the disruption of respiratory chain reactions the interaction of silver ions with DNA inhibits cell division,[19a,32] which ultimately leads to cell death.

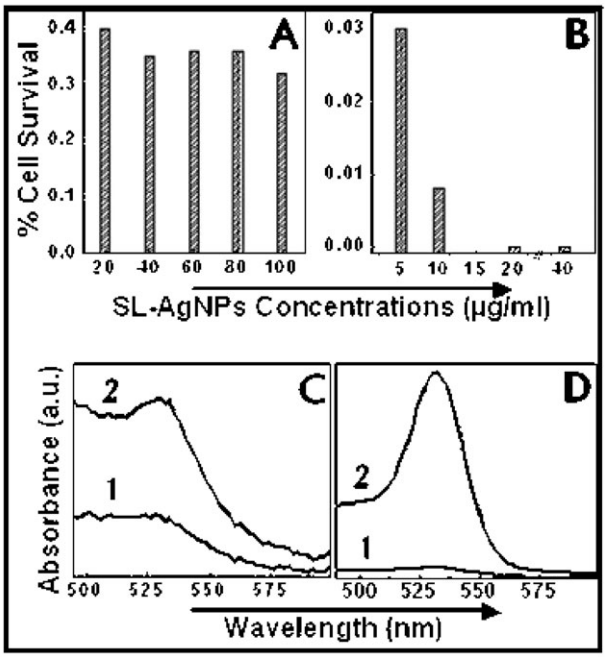

Fig. 4 Antibacterial activity of SL-AgNPs against *Bacillus subtilis* (A) and *Pseudomonas aeruginosa* (B) exposed for 1 h. The concentration given is the weight of sophorolipid capped silver particles mL^{-1} of the solution taken. Estimation of lipid peroxidation through release of malondialdehyde (MDA) in *Bacillus subtilis* (C) and *Pseudomonas aeruginosa* (D). The MDA treated with thiobarbituric acid (TBA) gives a pink adduct displaying absorbance maxima at 532 nm. Curve-1 and curve-2 in C and D are the absorbance spectra recorded from untreated and treated bacterial cells, respectively.

The ROS have been postulated to attack polyunsaturated phospholipids present in bacterial cell membrane through a lipid peroxidation (LPO) reaction process. Therefore, in order to probe the LPO process the release of malondialdehyde (MDA) was recorded in supernatant of bacterial cells treated with SL-AgNPs as compared to untreated (control) cells. It is clearly seen that in the case of treated cells (Fig. 4C and D, curve-2) the MDA released (seen as an adduct formed between MDA and thiobarbituric acid showing an intense band at 532 nm in UV-Vis spectra) is much higher as compared to the untreated cells (Fig. 4C and D, curve-1), thereby establishing this to be a cell wall destruction pathway. This would then pave the way for interaction of silver ions released from SL-AgNPs or the SL-AgNPs themselves with the essential molecules of cells like DNA and enzymes inhibiting the cell division *etc.* and finally to their death.

It is interesting to note the higher effectiveness of SL-AgNPs against Gram-negative bacteria as compared to Gram-positive

 This journal is © The Royal Society of Chemistry and the Centre National de la Recherche Scientifique 2009

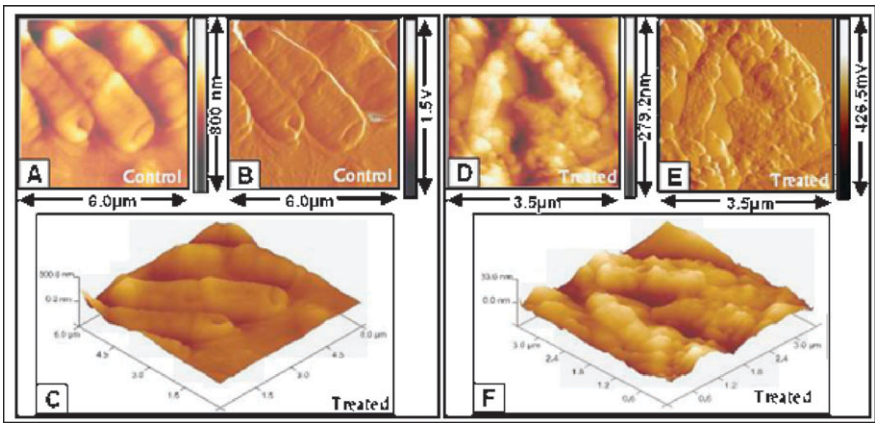

Fig. 5 AFM images revealing the antibacterial activity of SL-capped silver nanoparticles against *Bacillus subtilis*. Images in A and D show the height images while those in B and E are the deflexion counterparts. The 3D analyses of the images are displayed in C and F. Images A, B and C are of intact cells and those in D, E and F are after exposure to SL-capped silver nanoparticles.

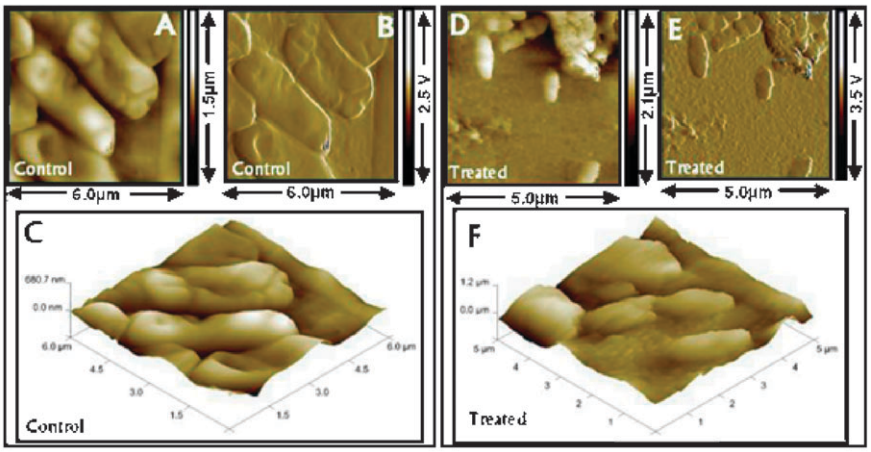

Fig. 6 AFM images revealing the antibacterial activity of SL-capped silver nanoparticles against *Pseudomonas aeruginosa*. Images in A and D show the height images while those in B and E are the deflection counterparts. The 3D analyses of the images are displayed in C and F. Images A, B and C are of intact cells and those in D, E and F are after exposure to SL-capped silver nanoparticles.

bacteria though in pure form SLs show lower activity towards Gram-negative bacteria. This may be attributed to the constitutional differences in the cell membrane. The Gram-negative bacteria are characterized by a thin peptidoglycan layer supported externally by an outer membrane made up of lipopolysaccharides and phospholipids. The SL capping may support a favourable interaction between these lipopolysaccharides/phospholipids and SL capped AgNPs. The presence of porin proteins in this outer layer probably allows a better passage of silver ions inside the bacterial cell once the AgNPs are close to the outer layer. The thin peptidoglycan layer is then accessible to SL-AgNPs, making it more susceptible to ROS attack and thus more vulnerable. Conversely, the peptidoglycan layer of Gram-positive bacteria is thicker and hence less vulnerable to the ROS thus requiring higher amounts of SL AgNPs for their killing.

To summarise, sophorolipids, an interesting class of glycolipids, are shown to reduce and act as *in situ* capping agents for the synthesis of stable and water dispersible AgNPs. Gratifyingly, these particles could be isolated simply as stable powder and could be re-dispersed in water with minor aggregation. Investigations presented here demonstrate these SL capped nanoparticles to be antibacterial agents against both Gram-positive and Gram-negative bacteria. Though the antibacterial effects are comparable to those of oleic acid capped silver nanoparticles the SL capping provides better stability in terms of the purification with centrifuging and drying and the re-dispersibility of the ensuing powder.

Acknowledgements

SS thanks CSIR (New Delhi) and PP thanks UGC (New Delhi) for financial support. The funding for this work by DBT *via* a project to AAP, CVR and BLVP and DST through the DST-UNANST scheme for NCL is gratefully acknowledged.

References

1 J. M. De la Fuente and S. Penades, *Biochim. Biophys. Acta*, 2006, **1760**, 636.
2 (*a*) J. M. De la Fuente, A. G. Barrientos, T. C. Rojas, J. Rojo, J. Canada, A. Fernandez and S. Penades, *Angew. Chem., Int. Ed.*, 2001, **40**, 2257; (*b*) A. G. Barrientos, J. M. De la Fuente,

Published on 12 December 2008 on http://pubs.rsc.org | doi:10.1039/B811829A
Downloaded by University of Belgrade on 02 January 2013

View Article Online

Published on 12 December 2008 on http://pubs.rsc.org | doi:10.1039/B811829A
Downloaded by University of Belgrade on 02 January 2013

T. C. Rojas, A. Fernandez and S. Penades, *Chem.–Eur. J.*, 2003, **9**, 1909; (*c*) C.-C. Lin, Y.-C. Yeh, C.-Y. Yang, G.-F. Chen, Y.-C. Chen, Y.-C. Wu and C.-C. Chen, *Chem. Commun.*, 2003, 2920; (*d*) A. C. De Souza, K. M. Halkes, J. D. Meeldijk, A. J. Verkleij, J. F. G. Vliegenthart and J. P. Kamerling, *Eur. J. Org. Chem.*, 2004, 4323; (*e*) K. M. Halkes, A. C. De Souza, C. E. P. Maljaars, G. J. Gerwig and J. P. Kamerling, *Eur. J. Org. Chem.*, 2005, 3650; (*f*) Y.-J. Chen, S.-H. Chen, Y.-Y. Chien, Y.-W. Chang, H.-K. Liao, C.-Y. Chang, M.-D. Jan, K.-T. Wang and C.-C. Lin, *ChemBioChem*, 2005, **6**, 1169.

3 J. M. de la Fuente, D. Alcántara and S. Penadés, *IEEE Trans. Nanobiosci.*, 2007, **6**, 275.

4 (*a*) Y. Chen, T. Ji and Z. Rosenzweig, *Nano Lett.*, 2003, **3**, 581; (*b*) X.-L. Sun, W. Cui, C. Haller and E. L. Chaikof, *ChemBioChem*, 2004, **5**, 1593; (*c*) J. M. de la Fuente and S. Penadés, *Tetrahedron: Asymmetry*, 2005, **16**, 387.

5 E. Katz and I. Willner, *Angew. Chem., Int. Ed.*, 2004, **43**, 6042.

6 (*a*) F. Furno, K. S. Morley, B. Wong, B. L. Sharp, P. L. Arnold, S. M. Howdle, R. Bayston, P. D. Brown, P. D. Winship and H. J. Reid, *J. Antimicrob. Chemother.*, 2004, **54**, 1019; (*b*) I. Sondi and B. Salopek-Sondi, *J. Colloid Interface Sci.*, 2004, **275**, 177; (*c*) J. R. Morones, J. L. Elechiguerra, A. Camacho, K. Holt, J. B. Kouri, J. T. Ramirez and M. Yacaman, *J. Nanotechnol.*, 2005, **16**, 2346.

7 P. Jain and T. Pradeep, *Biotechnol. Bioeng.*, 2005, **90**, 59.

8 (*a*) S. Tarimala, N. Kothari, N. Abidi, E. Hequet, J. Fralick and L. L. Dai, *J. Appl. Polym. Sci.*, 2006, **101**, 2938; (*b*) A. Melaiye, Z. Sun, K. Hindi, A. Milsted, D. Ely, D. H. Reneker, C. A. Tessier and W. J. Youngs, *J. Am. Chem. Soc.*, 2005, **127**, 2285.

9 J. L. Elechiguerra, J. L Burt, J. R. Morones, A. Camacho-Bragado, X. Gao, H. H. Lara and M. J. Yacaman, *J. Nanobiotechnol.*, 2005, 3. This paper can be accessed at http://www.jnanobiotechnology.com/content/3/1/6.

10 W. S. Choi, H. Y. Koo, J. Park and D. Kim, *J. Am. Chem. Soc.*, 2005, **127**, 16136.

11 (*a*) V. Sambhy, M. M. MacBride, B. R. Peterson and A. Sen, *J. Am. Chem. Soc.*, 2006, **128**, 9798; (*b*) W. S. Choi, H. Y Koo, J.-H. Park and D.-Y. Kim, *J. Am. Chem. Soc.*, 2005, **127**, 16136.

12 T. Hasell, J. Yang, W. Wang, P. D. Brown and S. M. Howdle, *Mater. Lett.*, 2007, **61**, 4906.

13 (*a*) N. Vigneshwaran, R. P. Nachane, R. H. Balasubramanya and P. V. Varadarajan, *Carbohydr. Res.*, 2006, **341**, 2012; (*b*) Y. Wang, J. F. Wong, X. Teng, X. Z. Lin and H. Yang, *Nano Lett.*, 2003, **3**, 1555; (*c*) S. Pande, S. K. Ghosh, S. Praharaj, S. Panigrahi, S. Basu, S. Jana, A. Pal, T. Tsukuda and T. Pal, *J. Phys. Chem. C*, 2007, **111**, 10806; (*d*) B. He, J. J. Tan, K. Y. Liew and H. Liu, *J. Mol. Catal. A: Chem.*, 2004, **221**, 121.

14 P. C. Lee and D. Meisel, *J. Phys. Chem.*, 1982, **86**, 3391.

15 J. A. Creighton, C. G. Blatchford and M. G. Albrecht, *J. Chem. Soc., Faraday Trans. 2*, 1979, **75**, 790.

16 D. Evanoff, Jr and G. Chumanov, *J. Phys. Chem. B*, 2004, **108**, 13948 and references cited therein.

17 (*a*) P. R. Selvakannan, S. Mandal, S. Phadtare, A. Gole, R. Pasricha, S. D. Adyanthaya and M. Sastry, *J. Colloid Interface Sci.*, 2004, **269**, 97; (*b*) P. R. Selvakannan, A. Swami, D. Srisathiyanarayanan, P. S. Shirude, R. Pasricha, A. B. Mandale and M. Sastry, *Langmuir*, 2004, **20**, 7825.

18 (*a*) B. Wiley, Y. Sun, B. Mayers and Y. Xia, *Chem.–Eur. J.*, 2005, **11**, 454; (*b*) B. Wiley, Y. Sun and Y. Xia, *Acc. Chem. Res.*, 2007, **40**, 1067.

19 (*a*) A. Panacek, L. Kvıtek, R. Prucek, M. Kolar, R. Vecerova, N. Pizurova, V. K. Sharma, T. Nevecna and R. Zboril, *J. Phys. Chem. B*, 2006, **110**, 16248; (*b*) Y. Saito, J. J. Wang, D. N. Batchelder and D. A. Smith, *Langmuir*, 2003, **19**, 6857; (*c*) Y. D. Yin, Z. Y. Li, Z. Y. Zhong, B. Gates, Y. N. Xia and S. Venkateswaran, *J. Mater. Chem.*, 2002, **12**, 522.

20 (*a*) I. N. A. Van Bogaert, K. Saerens, C. D. Muynck, D. Develter, W. Soetaert and E. J. Vandamme, *Appl. Microbiol. Biotechnol.*, 2007, **76**, 23; (*b*) M. Deshpande and L. Daniels, *Bioresour. Technol.*, 1995, **54**, 143; (*c*) J. D. Desai and I. M. Banat, *Microbiol. Mol. Biol. Rev.*, 1997, **61**, 47; (*d*) S. Ogawa and Y. Ota, *Biosci., Biotechnol., Biochem.*, 2000, **64**, 2466; (*e*) U. Rau, S. Hammen, R. Heckmann, V. Wray and S. Lang, *Ind. Crops Prod.*, 2001, **13**, 85; (*f*) D. Kitamoto, H. Isoda and T. Nakahara, *J. Biosci. Bioeng.*, 2002, **94**, 187; (*g*) R. S. Makkar and S. S. Cameotra, *Appl. Microbiol. Biotechnol.*, 2002, **58**, 428; (*h*) R. D. Ashby, D. K. Y. Solaiman and T. A. Foglia, *Biotechnol. Lett.*, 2006, **28**, 253; (*i*) B. Panilaitis, G. R. Castro, D. Solaiman and D. L. Kaplan, *J. Appl. Microbiol.*, 2007, **102**, 531.

21 (*a*) U. Rau, R. Heckmann, V. Wray and S. Lang, *Biotechnol. Lett.*, 1999, **21**, 973; (*b*) K. S. Bisht, R. A. Gross and D. L. Kaplan, *J. Org. Chem.*, 1999, **64**, 780; (*c*) E. Kandil, H. Zhang, R. Schulze, L. Dresner, M. Nowakowski, R. A. Gross and M. E. Zenilman, *J. Am. Coll. Surg.*, 2003, **197**, S40; (*d*) S. K. Singh, A. P. Felse, A. Nunez, T. A. Foglia and R. A. Gross, *J. Org. Chem.*, 2003, **68**, 5466; (*e*) S. Zhou, C. Xu, J. Wang, W. Gao, R. Akhverdiyeva, V. Shah and R. Gross, *Langmuir*, 2004, **20**, 7926; (*f*) V. Shah, G. F. Doncel, T. Seyoum, K. M. Eaton, I. Zalenskaya, R. Hagver, A. Azim and R. Gross, *Antimicrob. Agents Chemother.*, 2005, **49**, 4093; (*g*) A. Azim, V. Shah, G. F. Doncel, N. Peterson, W. Gao and R. Gross, *Bioconjugate Chem.*, 2006, **17**, 1523; (*h*) V. Shah, M. Jurjevic and D. Badia, *Biotechnol. Prog.*, 2007, **23**, 512; (*i*) V. Shah, D. Badia and P. Ratsep, *Antimicrob. Agents Chemother.*, 2007, **51**, 397.

22 M. Kasture, S. Singh, P. Patel, P. A. Joy, A. A. Prabhune, C. V. Ramana and B. L. V. Prasad, *Langmuir*, 2007, **23**, 11409.

23 H. Esterbauer and K. H. Cheeseman, *Methods Enzymol.*, 1990, **186B**, 407.

24 (*a*) U. Kreibig and M. Vollmer, *Optical Properties of Metal Clusters*, Springer-Verlag, Berlin, 1995, Springer Series in Materials Science, vol. 25; (*b*) P. Mulvaney, *Langmuir*, 1996, **12**, 788.

25 The XRD patterns were indexed with reference to the crystal structures from the ASTM chart no. 04-0783.

26 (*a*) W. D. Luedtke and U. Landman, *J. Phys. Chem.*, 1996, **100**, 13323; (*b*) W. D. Luedtke and U. Landman, *J. Phys. Chem. B*, 1998, **102**, 6566.

27 (*a*) W. Wang, S. Efrima and O. Regev, *Langmuir*, 1998, **14**, 602; (*b*) W. Wang, X. Chen and S. Efrima, *J. Phys. Chem. B*, 1999, **103**, 7238; (*c*) T. Bala, A. Swami, B. L. V. Prasad and M. Sastry, *J. Colloid Interface Sci.*, 2005, **283**, 422.

28 Such down shielded proton signals have been observed previously in thiol bound metal nanoparticle cases and are attributed to the proximity of these protons to the metal surface. (*a*) R. H. Terril, T. A. Postlethwaite, C.-H. Chen, C.-D. Poon, A. Terzis, A. Chen, J. E. Hutchison, M. R. Clark, G. Wignall, J. D. Londono, R. Superfine, M. Flavo, C. S. Johnson, Jr, E. T. Samulski and R. W. Murray, *J. Am. Chem. Soc.*, 1995, **117**, 12537; (*b*) A. Badia, S. Singh, L. Demers, L. Cuccia, G. R. Brown and R. B. Lennox, *Chem.–Eur. J.*, 1996, **2**, 359; (*c*) M. Hasan, D. Bethell and M. Brust, *J. Am. Chem. Soc.*, 2002, **124**, 1132; (*d*) A. Badia, W. Gao, S. Singh, L. Demers, L. Cuccia and L. Reven, *Langmuir*, 1996, **12**, 1262; (*e*) A. Kumar, S. Mandal, P. R. Selvakannan, R. Pasricha, A. B. Mandale and M. Sastry, *Langmuir*, 2003, **19**, 6277; (*f*) D. V. Leff, L. Brandt and J. R. Heath, *Langmuir*, 1996, **12**, 4723.

29 (*a*) H. Hirai, H. Aizawa and H. Shiozaki, *Chem. Lett.*, 1992, 1527; (*b*) H. Hirai and H. Aizawa, *J. Colloid Interface Sci.*, 1993, **161**, 471.

30 M. Meincken, D. L. Holroyd and M. Rautenbach, *Antimicrob. Agents Chemother.*, 2005, **49**, 4085.

31 (*a*) I. Sondi and B. Salopek-Sondi, *J. Colloid Interface Sci.*, 2004, **275**, 177; (*b*) P.-C. Maness, S. Smolinski, D. M. Blake, Z. Huang, E. J. Wolfrum and W. A. Jacoby, *Appl. Environ. Microbiol.*, 1999, **65**, 4094.

32 (*a*) A. B. Smetana, K. J. Klabunde, G. R. Marchin and C. M. Sorensen, *Langmuir*, 2008, **24**, 7457; (*b*) G. L. Feng, J. Wu, G. Q. Chen, F. Z. Cui, T. M. Kim and O. J. Kim, *J. Biomed. Mater. Res.*, 2000, **52**, 662; (*c*) K. B. Holt and A. J. Bard, *Biochemistry*, 2005, **44**, 13214; (*d*) D. W. Hatchett and S. Henry, *J. Phys. Chem.*, 1996, **100**, 9854; (*e*) T. Vitanov and A. Popov, *J. Electroanal. Chem.*, 1983, **159**, 437; (*f*) S. Ahrland, J. Chatt and N. R. Davies, *Q. Rev. Chem. Soc.*, 1958, **12**, 265; (*g*) I. E. Alcamo, *Fundamentals of Microbiology*, Addison Wesley Longman Inc., Reading, MA, 1997, 5th edn; (*h*) Q. L. Feng, J. Wu, G. Q. Chen, F. Z. Cui, T. N. Kim and J. O. Kim, *J. Biomed. Mater. Res.*, 2000, **52**, 662; (*i*) J. R. Morones, J. L. Elechiguerra, A. Camacho, K. Holt, J. Kouri, J. T. Ramirez and M. J. Yacaman, *Nanotechnology*, 2005, **16**, 2346; (*j*) S. K. Gogoi, P. Gopinath, A. Paul, A. Ramesh, S. S. Ghosh and A. Chattopadhyay, *Langmuir*, 2006, **22**, 9322.

 This journal is © The Royal Society of Chemistry and the Centre National de la Recherche Scientifique 2009